THE ASTROPHYSICAL JOURNAL, 490:452–457, 1997 November 20

INFERENCE OF SUBSURFACE MAGNETIC FIELD OF SUNSPOTS FROM ABSORPTION COEFFICIENTS OF *p*-MODES IN SUNSPOTS

HUEI-RU CHEN, DEAN-YI CHOU, AND THE TON TEAM[1]
Physics Department, Tsing Hua University, Hsinchu, 30043, Taiwan, Republic of China
Received 1997 March 13; accepted 1997 July 3

ABSTRACT

The interaction of *p*-mode waves with an active region can be described by a phenomenological parameter, hereafter called the interaction parameter. The measured absorption coefficients of *p*-modes relate to the interaction parameter by Chou et al.'s an integral equation. We assume that the sunspot is axisymmetric and the interaction parameter is uniform in the horizontal direction inside the sunspot. The depth dependence of the sunspot radius is given in our study. Thus, the problem becomes one-dimensional: to determine the interaction parameter versus depth. We use the optimally localized averages method to invert the absorption coefficients, measured with the Taiwan Oscillation Network data and South Pole data, to infer the interaction parameter versus depth. For two sunspots we have studied, the depth dependences of the interaction parameter are similar: the interaction parameter increases rapidly, as depth increases, to a maximum value at a depth of about of 7 Mm, and then gradually drops to zero at a depth of about 28–35 Mm. The distribution of the interaction parameter also depends on the depth variation of sunspot radius in such a way that the interaction parameter anticorrelates with the sunspot radius.

Subject headings: Sun: magnetic field — Sun: oscillations — sunspots

1. INTRODUCTION

Local analyses of helioseismic data have shown that a sunspot would modify the amplitude and phase of *p*-mode waves as the waves pass through the sunspot (Braun, Duvall, & LaBonte 1987; Braun et al. 1992; Braun 1995). The interaction between the waves and magnetic field provides a tool for probing the properties of a sunspot, such as magnetic field, density, and temperature, below the surface. Many theoretical models have been proposed to study the interaction mechanisms responsible for this phenomenon (see the review by Bogdan & Braun 1995). However, it is difficult to compute the amplitude changes and phase shifts directly from the theory of interaction mechanism and compare with measurements. Several phenomenological models using scattering theory have been proposed to bridge measured quantities—absorption coefficients and phase shifts—and the physical mechanisms (Brown 1990; Chou 1994; Fan, Braun, & Chou 1995; Chou et al. 1996). In this study we will use the phenomenological model proposed by Chou et al. (1996, hereafter Paper I) and the measured absorption coefficients to infer the subsurface magnetic structure of sunspots. In this model, the interaction of *p*-mode waves with an active region is described by a phenomenological parameter, hereafter called the interaction parameter. The interaction parameter should relate to the distribution of a magnetic field that requires a theory of interaction mechanism. The measured absorption coefficient of *p*-modes relates to the interaction parameter by an integral equation. We use the optimally localized averages method to invert the measured absorption coefficients to infer the distribution of the interaction parameter below the surface (Chen et al. 1997; Chou & the TON Team 1997). In this paper, we study two sunspots: NOAA 5254 and NOAA 7887. The absorption coefficients of NOAA 5254 are analyzed by Braun (1995) from 67.7 hr data taken at South Pole. The absorption coefficients of NOAA 7887 are measured by us from 100.4 hr data taken by Taiwan Oscillation Network (TON) (Chou et al. 1995). In § 2, we briefly describe the phenomenological model to be used for the inversion. In § 3, we describe how absorption coefficients are measured. In § 4, we discuss optimally localized averages method used for the inversion. In § 5, we discuss the results.

2. PHENOMENOLOGICAL MODEL

The discussion in this section basically follows that of Paper I. In the phenomenological model proposed in Paper I, the interaction of *p*-mode waves with a sunspot is described by introducing a complex sound speed,

$$c^2 = \frac{c_0^2}{1 - i\sigma}, \tag{1}$$

where c_0 is the sound speed in nonmagnetic regions. The dimensionless parameter σ is called the interaction param-

[1] The TON Team includes: Ming-Tsung Sun (Department of Mechanical Engineering, Chang-Gung College of Medical and Technology, Kwei-San, Taiwan, Republic of China); Tao-Mo Mu, Chia-Hsien Lin, Said Loudagh, B. Bala, and I-Jen Huang (Physics Department, Tsing Hua University, Hsinchu, 30043, Taiwan, Republic of China); Antonio Jimenez and Maria Cristina Rabello-Soares (Instituto Astrofisica de Canarias, Observatorio del Teide, Tenerife, Spain); Guoxiang Ai and Gwo-Ping Wang (Huairou Solar Observing Station, Beijing Observatory, Beijing, China); Harold Zirin and William Marquette (Big Bear Solar Observatory, California Institute of Technology, Pasadena, CA 91125); Shuhrat Ehgamberdiev and Shukur Khalikov (Ulugh Beg Astronomical Institute, Tashkent, Uzbekistan).

eter and is related to the index of refraction n by $n = (1 - i\sigma)^{1/2}$. Here all three quantities, c_0, c, and σ, depend on the position. In general, σ is a complex number. If σ is small compared with unity, to the lowest order, the real part of σ corresponds to the dissipation of waves and the imaginary part describes the change of the phase velocity due to the change of physical conditions in magnetic regions. In this paper, we assume that σ is small and use only measured absorption coefficients to invert the real part of σ. Our results show that this assumption is a good approximation. Hereafter, we will use the magnetic region, the sunspot, and the absorption region interchangeably.

To make the problem tractable, we will assume that the sunspot (distribution of σ in the horizontal direction) is uniform and axisymmetric. For such a sunspot, the coupling among different modes is small. The absorption coefficient α can be approximately expressed as (Paper I)

$$\alpha_{nkm} \approx -i \frac{2\pi}{\omega_{nk}^2} \left(\frac{k}{\omega_{nk}} \frac{\partial \omega_{nk}}{\partial k} \right)^{-1} \int N_{km}(z) \sigma(z) Z_{nk}(z) dz \ , \quad (2)$$

where $N_{km}(z) \equiv \int_0^{ka(z)} x |J_m(x)|^2 dx$ and the kernel $Z_{nk}(z)$ is a functional of wave function in z-direction. In general, the radius of the sunspot, a, depends on the depth. To derive equation (2), we have used cylindrical coordinates. In measuring absorption coefficients, we use spherical coordinates. Since we focus on a small region near the sunspot, the vertical coordinate z in equation (2) can be replaced by the radial coordinate r and the horizontal wavenumber k by the harmonic degree l with $k = [l(l+1)]^{1/2}/R$, where R is the solar radius. In general, the sunspot radius a depends on the depth, and the problem is two-dimensional. To reduce the complication, in this paper we assume that $a(z)$ is given and study two cases: (i) $a(z)$ is constant in z, and (ii) $a(z)$ is a given funnel shape. Thus, the problem is reduced to one-dimension: to determine σ versus z. The comparison of $\sigma(z)$ derived from above two cases would give us some ideas how $\sigma(z)$ varies with $a(z)$.

3. MEASUREMENTS OF ABSORPTION COEFFICIENTS

The absorption coefficient α_{nlm} is defined as the fraction of energy of incident waves absorbed by the sunspot. It can be measured by decomposing the p-mode oscillations around a sunspot into the modes propagating toward and away from the sunspot (Braun et al. 1987; Bogdan et al. 1993; Chen, Chou, & the TON Team 1996). Here we study two active regions: NOAA 5254 and NOAA 7887.

The absorption coefficients of NOAA 5254, shown in Figure 1, are measured by Braun (1995) from 67.7 hr data taken at South Pole. NOAA 5254 has a dominant sunspot with several small sunspots. The annulus used to measure the absorption coefficients is centered at the center of the dominant sunspot, which has a penumbra radius of 18 Mm. The annular region used to measure the absorption coefficients is 2°.5–20°. So the resolution in l, Δl, is about 20. The data reduction procedure to measure the absorption coefficients of NOAA 5254 is described by Braun (1995). The absorption coefficients of NOAA 7887, shown in Figure 2, are measured by us from 100.4 hr data taken with the TON telescopes at Tenerife and Big Bear (Chen et al. 1997). NOAA 7887 is an old active region and has only one sunspot, which has a penumbra radius of 16.4 Mm. The annular region used to measure the absorption coefficients is 2°–10°. The corresponding Δl is 45. The procedure to measure the coefficients from TON data is described by Chen et al. (1996).

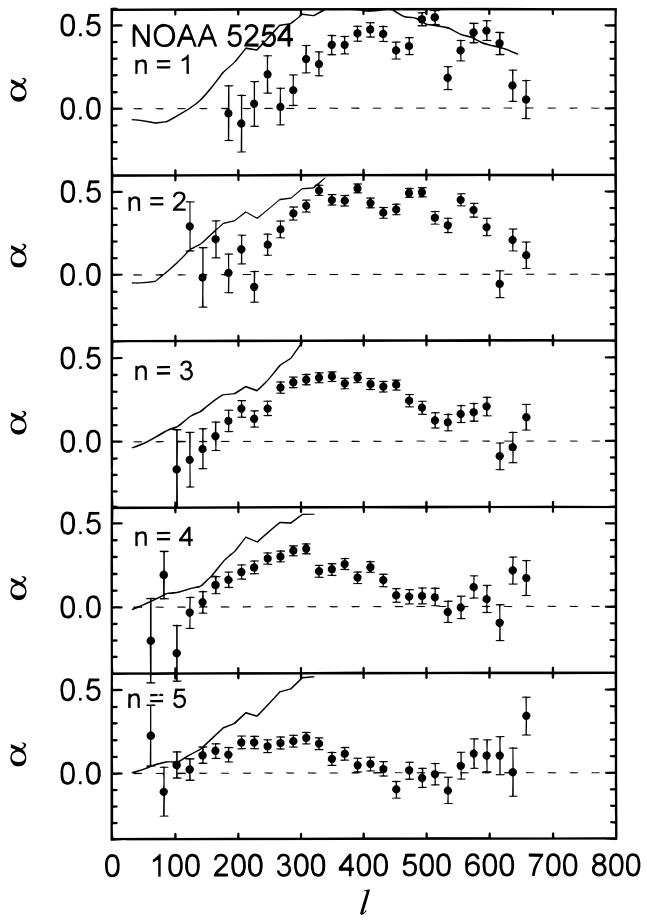

FIG. 1.—Absorption coefficients α_{nl} of NOAA 5254 vs. l for $n = 1$–5. Dots were measured by Braun (1995) from 67.7 hr data taken at the South Pole. Curves are computed from $\langle \sigma \rangle$ in the upper panel of Fig. 4 based on eq. (3).

To increase the signal-to-noise ratio, α_{nl} is computed by summing power over m up to a critical value m_{cr} that is described in Braun (1995) and Chen et al. (1996). The measured absorption coefficients α_{nl} for NOAA 5254 and 7887 are shown in Figures 1 and 2, respectively, for $n = 1$–5. Equation (2) can be approximated by

$$\alpha_{nl} \approx -i \frac{2\pi}{\omega_{nl}^2} \left(\frac{l}{\omega_{nl}} \frac{\partial \omega_{nl}}{\partial l} \right)^{-1} \int \bar{N}_l(r) \sigma(r) Z_{nl}(r) dr \ , \quad (3)$$

where $\bar{N}_l(r)$ is the average of $N_{lm}(r)$ over m up to m_{cr}. In equation (3), we have replaced k by l and z by r.

To use the optimally localized averages method, we need modes more than those shown in Figures 1 and 2 to form localized kernels. Thus, we have to interpolate the measured α_{nl} to obtain α_{nl} for other modes. First, we smooth the measured α_{nl} by a five-point running mean. Second, we interpolate the measured α_{nl} to obtain α_{nl} for every four l for NOAA 5254 and every five l for NOAA 7887. Figures 1 and 2 and other observations (Braun et al. 1987; Chen 1995) show that α_{nl} becomes zero for small l. The l value where α_{nl} becomes zero depends on the depth of the lower boundary of the absorption region. To determine the depth where σ vanishes from the inversion, we need α_{nl} at low l. Thus, we extend the data of α_{nl} to $l = 32$ for NOAA 5254 and $l = 31$ for NOAA 7887 by assigning a value of zero to α_{nl} for l

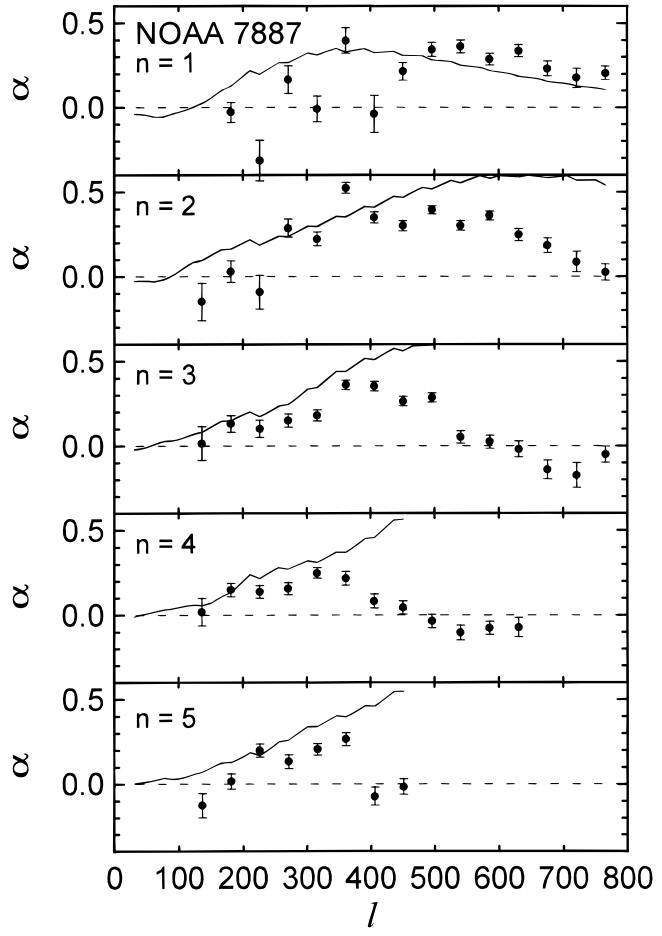

FIG. 2.—Absorption coefficients α_{nl} of NOAA 7887 vs. l for $n = 1$–5. Dots are measured by us from 100.4 hr data taken by the Taiwan Oscillation Network. Curves are computed from $\langle\sigma\rangle$ in the upper panel of Fig. 5 based on eq. (3).

smaller than the observing range. The errors of α_{nl} are also smoothed and interpolated accordingly.

4. INVERSION METHOD

Equation (3) can be written as

$$\alpha_i = \int K_i(r)\sigma(r)dr + \epsilon_i \,, \tag{4}$$

where the subscript i denotes the mode (n, l) and K_i is the corresponding kernel. Here we introduce the error in the measurement, ϵ_i, which is Gaussian distributed with zero mean. The goal of this study is to invert the measured absorption coefficients α_i in equation (4) to obtain the depth dependence of σ. Here we use the optimally localized averages method (Christensen-Dalsgaard, Schou, & Thompson 1990; Gough & Thompson 1991; Pijpers & Thompson 1992). The basic idea of the optimally localized averages method is, for a given depth r_0, to choose a linear combination of kernels K_i that is close to a delta function $\delta(r - r_0)$ so that the estimate of σ at r_0 can be easily evaluated. If the desired averaging kernel $\tilde{K}(r, r_0)$ is

$$\tilde{K}(r, r_0) \equiv \sum_i c_i(r_0)K_i(r) \,, \tag{5}$$

from equation (3) we have

$$\sum_i c_i(r_0)\alpha_i = \int_0^R \tilde{K}(r, r_0)\sigma(r)dr + \sum_i c_i(r_0)\epsilon_i \,. \tag{6}$$

The left-hand side, defined as $\langle\sigma(r_0)\rangle$, is an estimate of σ at $r = r_0$. The last term is the error, which is Gaussian distributed with zero mean and variance $\sum E_{ij}c_i(r_0)c_j(r_0)$, where $E_{ij} = \epsilon_i\epsilon_j\delta_{ij}$.

To choose coefficients $c_i(r_0)$, we have to make not only the averaging kernel $\tilde{K}_i(r, r_0)$ as close to $\delta(r - r_0)$ as possible but also the variance of error as small as possible. Following most authors in helioseismology, we minimize the quantity

$$12\int_0^R (r - r_0)^2[\tilde{K}(r, r_0)]^2dr + \mu \tan\theta \sum_{i,j} E_{ij}c_i(r_0)c_j(r_0) \,, \tag{7}$$

subject to

$$\int_0^R \tilde{K}(r, r_0)dr \equiv \sum_i c_i(r_0)\int_0^R K_i(r)dr = 1 \,. \tag{8}$$

Here the first term in equation (7) represents the spread of the averaging kernel $K(r, r_0)$, and the second term is the variance of the error. The parameter μ is given by $\sum_i E_{ii}/M$, where M is the number of modes in the summation. The trade-off parameter θ determines the relative desirability of making the first and second terms in equation (7) small.

To minimize the quantity in equation (7) with a constraint, equation (8), we introduce the Lagrange multiplier λ. Then coefficients c_i are determined by

$$\sum_j \left[12\int_0^R (r - r_0)^2K_iK_j\,dr + \mu \tan\theta E_{ij}\right] \times c_j(r_0) + \frac{1}{2}\lambda\int_0^R K_i\,dr = 0 \,, \tag{9}$$

for $i = 1, \ldots, M$, together with equation (8). Solving this set of $M + 1$ linear coupled algebraic equations yields M coefficients c_i and the parameter λ.

5. RESULTS AND DISCUSSION

In equation (3), the sunspot radius $a(r)$ is hidden in $\bar{N}_l(r)$, which depends on l. It is difficult to obtain the depth dependence of a from inversion. Thus, in this study we assume that $a(r)$ is given to reduce the problem to one-dimension: to determine the depth dependence of $\langle\sigma\rangle$ from the measured α_{nl}. The simplest case is that the sunspot has a cylindrical shape; i.e., a is constant in r. Then $\bar{N}_l$ is independent of r and can be taken out of the integral in equation (3). The kernel of each mode K_i is a functional of the mode wave function (Paper I). The mode wave functions are computed by the computer codes provided by Y. Gu (private communication, 1993) and by Christensen-Dalsgaard's solar model. The coefficients $c_i(r_0)$ are then computed by the inversion method described in § 4. The averaging kernels, $\tilde{K}(r, r_0)$, at 10 different depths are shown in Figure 3 for NOAA 5254 and 7887. These averaging kernels correspond to $\langle\sigma\rangle$ shown in the upper panels of Figures 4 and 5. The complication of wave functions near the surface would cause $\tilde{K}(r, r_0)$ to rapidly oscillate near the surface. However, the contribution of $\tilde{K}(r, r_0)$ near the surface is estimated to be less than 1% in the integral if $r_0 < 0.995R$. The estimate of interaction parameter $\langle\sigma\rangle$ from inversion for NOAA

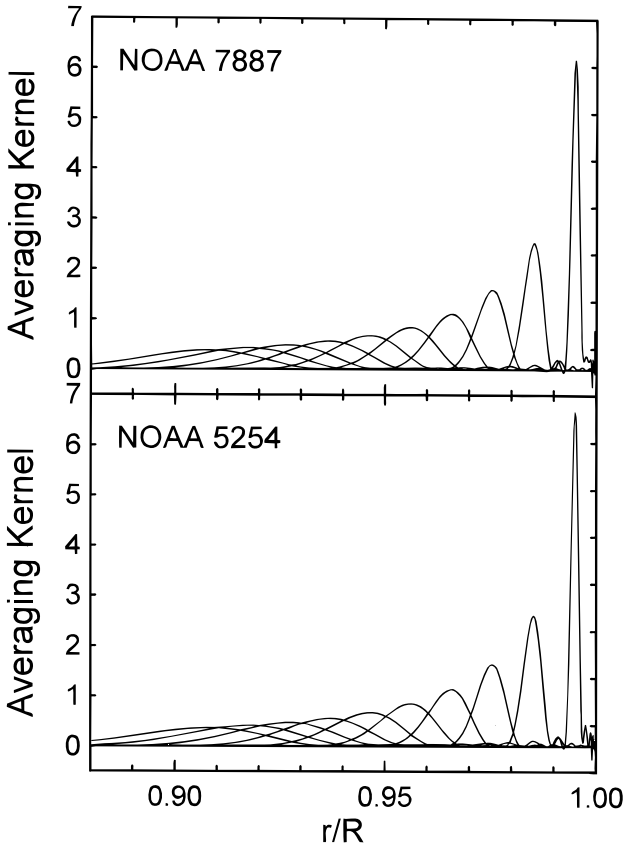

FIG. 3.—Averaging kernels at different depths for NOAA 7887 (*upper panel*) and NOAA 5254 (*lower panel*). These averaging kernels correspond to $\langle\sigma\rangle$ shown in the upper panels of Figs. 4 and 5.

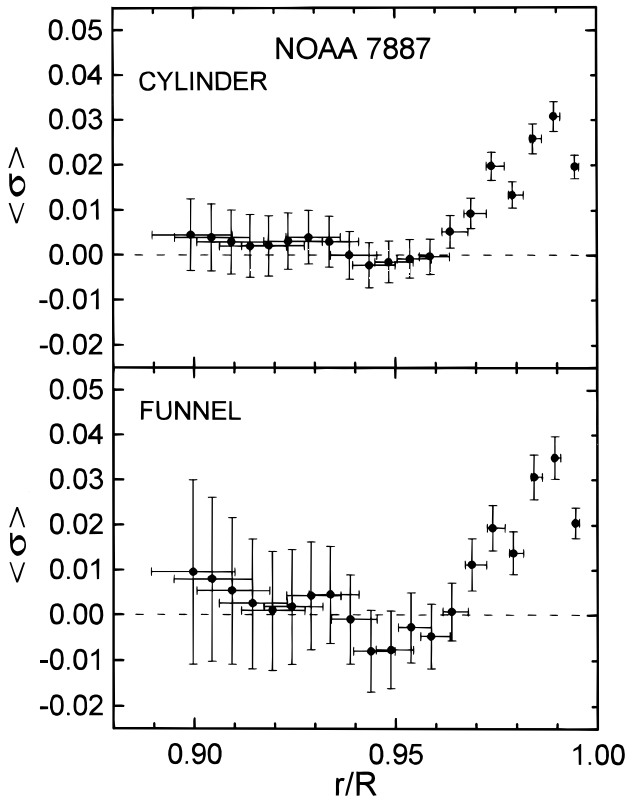

FIG. 5.—$\langle\sigma\rangle$ vs. r/R for NOAA 7887. The upper panel is for the sunspot with a constant radius of 16.4 Mm. The lower panel is for the funnel-shaped sunspot, defined in the text. The horizontal bar indicates the width of the averaging kernel.

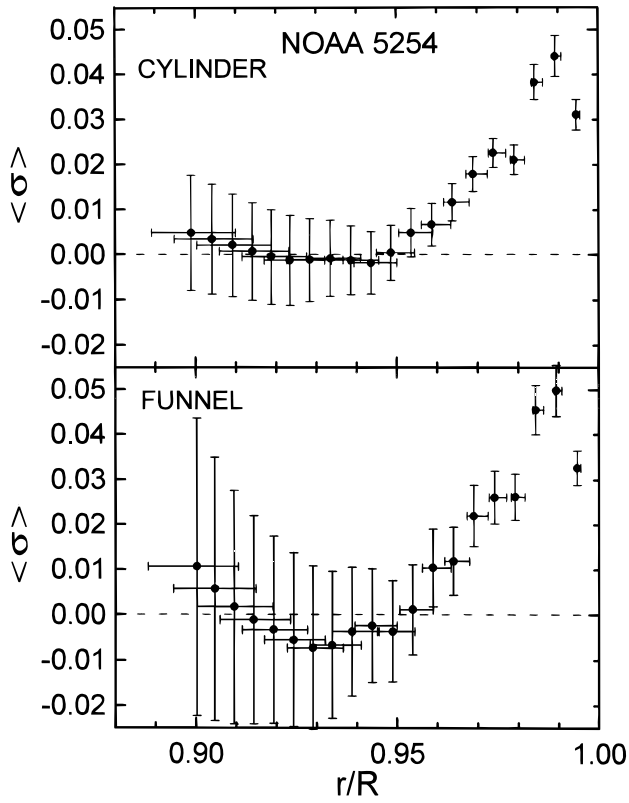

FIG. 4.—$\langle\sigma\rangle$ vs. r/R for NOAA 5254. The upper panel is for the sunspot with a constant radius of 18 Mm. The lower panel is for the funnel-shaped sunspot, defined in the text. The horizontal bar indicates the width of the averaging kernel.

7887 and 5254 is shown in the upper panels of Figures 4 and 5, respectively. The horizontal bar of the data point represents the width of the averaging kernel. For the results in Figures 4 and 5, we have set the trade-off parameter θ equal to 1 rad in equation (9). We have tried different θ's in a range of 0.5–1.5. They all give the similar $\langle\sigma\rangle$, although the error bars of $\langle\sigma\rangle$ are greater and the widths of $\tilde{K}(r, r_0)$ are smaller for the smaller θ, as expected.

Constructing the averaging kernels, $\tilde{K}(r, r_0)$, will fail for $r_0 > 0.995R$ in the sense that the sidelobes of $\tilde{K}(r, r_0)$ are not negligible, because the l value of modes used to construct $\tilde{K}(r, r_0)$ is not high enough, and r_0 will be in the evanescent regions for most modes if it is too close to R.

The value of $\langle\sigma\rangle$ depends on a. In this study, we set a to the radius of penumbra, which is 18 Mm for NOAA 5254 and 16.4 Mm for NOAA 7887. Figures 4 and 5 show that the distributions of $\langle\sigma\rangle$ for two regions have a surprisingly similar trend, although their values are slightly different. As the depth increases, $\langle\sigma\rangle$ increases rapidly to a maximum at a depth of about $0.01R$ (7 Mm), and then gradually drops to zero at a depth of about 0.04–$0.05R$ (28–35 Mm), which corresponds to the depth of the absorption region. The value of $\langle\sigma\rangle$ of NOAA 5254 is slightly greater than that of NOAA 7887. To see the effect of the value of a on $\langle\sigma\rangle$, we compare $\langle\sigma\rangle$ derived from different a. The upper panel of Figure 6 shows $\langle\sigma\rangle$ for $a = 12.3$, 16.4, and 20.5 Mm for NOAA 7887, and the lower panel shows $\langle\sigma\rangle$ for $a = 13.5$, 18, and 22.5 Mm for NOAA 5254. The distribution of $\langle\sigma\rangle$ is approximately scaled by a constant as a varies. This can be understood as in equation (3) a appears only in $\bar{N}_l$, and $\bar{N}_l$ is independent of r and insensitive to l.

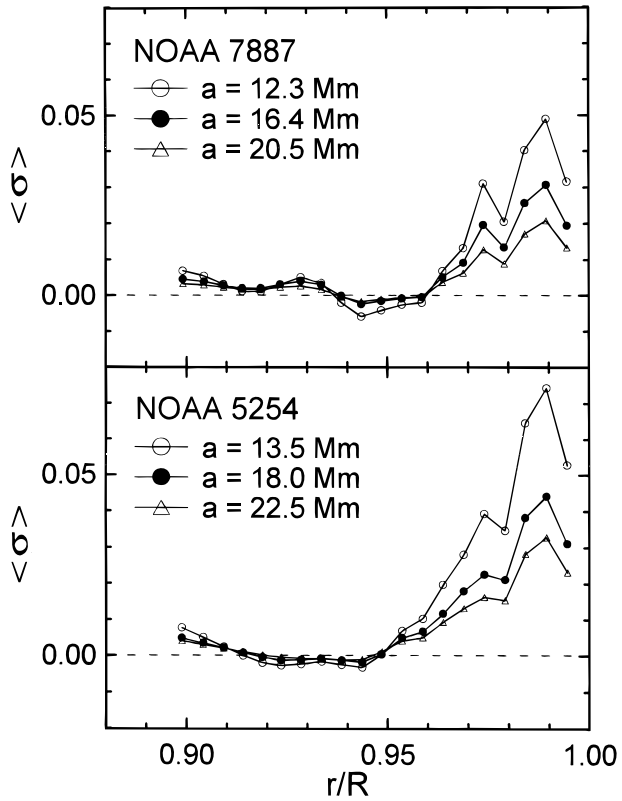

FIG. 6.—Comparison of $\langle\sigma\rangle$ derived from different constant sunspot radii for NOAA 7887 (*upper panel*) and 5254 (*lower panel*). Here we omit error bars to avoid the overlap.

The second case we study is a funnel-shaped sunspot. The r dependence of the sunspot radius is given by $a(r) = a(R)(r/R)^6$. The sunspot radius drops to $0.53a(R)$ at $r = 0.9R$. We set the sunspot radius on the surface, $a(R)$, to the radius of penumbra. The results for the funnel-shaped sunspot are shown in the lower panels of Figures 4 and 5. It is apparent that the absolute value of σ is larger for the funnel-shaped sunspot. The amplification anticorrelates with $a(r)$. This result is expected because a greater $\langle\sigma\rangle$ is required to compensate the small sunspot radius for generating the same measured α_{nl}. This comparison gives us an idea how the distribution of $\langle\sigma\rangle$ would change if the vertical shape of the sunspot were to change. The change of the vertical shape of the sunspot has little effect on the depth of the absorption region. The depth of the absorption region derived here for NOAA 5254 and 7887, about 28–35 Mm, is consistent with the result of Paper I, where the depth of the absorption region is estimated by comparing forward calculations with measured α_{nl}. Recently, Chang et al. (1997) used time-distance relations to construct a set of two-dimensional acoustic images of an area including a sunspot at different depths. They found that the acoustic intensity suppression inside the sunspot disappears at a depth of about 40 Mm.

Another sunspot model commonly adopted is that β (the ratio of gas pressure to magnetic pressure) is constant in depth inside the sunspot. In this model, $a(r) \propto p(r)^{-1/4}$, where p is the pressure. We did not succeed in constructing a localized averaging kernel for this model because the spot radius decreases very rapidly with depth. The spot radius decreases by 2 orders of magnitude from R to $0.96R$, which causes the contribution of the kernel of each mode to decrease very rapidly with depth. This rapid decrease of the individual kernel prevents us from constructing a localized averaging kernel. Although our inability to construct a localized averaging kernel is of no concern to the existence of such a sunspot model, we will argue that the radius of a real sunspot is unlikely to decrease as rapidly as this model that follows. First, this model is true only when the interior and exterior of the sunspot reach the thermal equilibrium. However, it is known that the temperature of the sunspot is lower than that of its surroundings, at least near the surface. This leads to an increase of β with depth and a less rapid decrease for the spot radius. Second, from the acoustic images in the solar interior (Chang et al. 1997), the size of the p-mode absorption region does not have a significant change in depth down to a depth of 30 Mm. Therefore, we tend to believe that Parker's fibril model, where β is constant in depth inside the fibrils while the overall cylindrical size of the sunspot has little change in depth, is closer to a real sunspot. The fibril model is also consistent with the result from the forward computation in Paper I. If the effective p-mode absorption in the fibril model can be described by a horizontally uniform σ inside the sunspot, the result of our cylindrical model can be applied to the fibril model to give the horizontally averaged σ as a function of depth. But the method discussed in this paper cannot distinguish the fibril sunspot model from the uniform cylindrical sunspot model.

It is interesting to compute α_{nl} corresponding to $\langle\sigma\rangle$ in Figures 4 and 5 with equation (3). Since we do not have information for $\langle\sigma\rangle$ beyond $0.995R$, we set $\langle\sigma\rangle = 0$ for $r > 0.995R$ in computing α_{nl}. The computed α_{nl} for the cylinder and funnel are close, and we show only the result for the cylinder in Figures 1 and 2. The computed α_{nl} continues to increase with l beyond the range of Figures 1 and 2 for high n. The discrepancy between the computed α_{nl} and the measured one increases with n and l because the mode cavity includes more and more regions above $0.995R$, where we do not have correct $\langle\sigma\rangle$, as n and l increase. We have tried different extrapolations for $\langle\sigma\rangle$ beyond $0.995R$. We found that the computed α_{nl} are sensitive to the value of $\langle\sigma\rangle$ at $r > 0.995R$, and we did not succeed in reproducing the measured α_{nl} by the extrapolations we have tried. For $r_0 < 0.995R$, $\tilde{K}(r, r_0)$ is mainly constructed with the lower-l modes, where the computed α_{nl} is in better agreement with measured one. Thus, it is not a surprise to have a large discrepancy between the computed α_{nl} and the measured one for high n and high l, if we set $\langle\sigma\rangle = 0$ for $r > 0.995R$. This together with the fact that constructing $\tilde{K}(r, r_0)$ fails as r_0 is close to R indicates that the method discussed in this paper can not provide information near the surface.

It should be emphasized that the distribution of σ represents the absorption region of p-modes in magnetic regions. The absorption of p-modes may depend not only on the magnetic field strength but also on the orientation of magnetic field and the p-mode propagation direction. Thus, the distribution of σ is not directly related to the field strength. On the other hand, the phase shift, which depends on the sound speed, is more directly related to the field strength. The phase shift corresponds to the imaginary part of σ. The method discussed in this paper can also apply to invert measured phase shifts. Finally, it should be mentioned that the finite lifetime of p-modes is not taken into account in this study. The effects of finite lifetime on this study are (i) the measured α_{nl} is smaller than its actual value,

especially for higher-l modes, and (ii) the measured α_{nl} depends on the size of the annulus used to measure it (Chen et al. 1996).

We are grateful to S. Basu for helpful discussions on inversion methods. We thank Y. Gu for providing the codes to compute eigenfunctions of p-modes. We also thank D. Braun for providing the data of the absorption coefficients of NOAA 5254. The TON project is supported by the National Science Council, Republic of China, under grants NSC-86-2112-M-007-036 and NSC-86-2112-M-182-003.

REFERENCES

Bogdan, T. J., & Braun, D. C. 1995, in Proc. 4th SOHO Workshop: Helioseismology, ed. V. Domingo et al. (ESA SP-376; Noordwijk: ESA), 31
Bogdan, T. J., Brown, T. B., Lite, B. W., & Thomas, J. H. 1993, ApJ, 406, 723
Braun, D. C. 1995, ApJ, 451, 859
Braun, D. C., Duvall, T. L., Jr., & LaBonte, B. J. 1987, ApJ, 319, L27
Braun, D. C., Duvall, T. L., Jr., LaBonte, B. J., Jefferies, S. M., Harvey, J. W., & Pomerantz, M. A. 1992, ApJ, 391, L113
Brown, T. M. 1990, Sol. Phys., 128, 133
Chang, H.-K., Chou, D.-Y., LaBonte, B., & the TON Team. 1997, Nature, in press
Chen, H.-R., Chou, D.-Y., Lin, C.-H., & the TON Team. 1997, in IAU Symp. 181, Sounding Solar and Stellar Interiors, ed. J. Provost, F. X. Schmider, & G. Berthomieu (Dordrecht: Kluwer), in press
Chen, K.-R. 1995, M.S. thesis, Tsing Hua Univ.
Chen, K.-R., Chou, D.-Y., & the TON Team. 1996, ApJ, 465, 985
Chou, D.-Y., Chou, H.-Y., Hsieh, Y.-C., & Chen, C.-K. 1996, ApJ, 459, 792 (Paper I)
Chou, D.-Y., et al. 1995, Sol. Phys., 160, 237
Chou, D.-Y., & the TON Team. 1997, in IAU Symp. 181, Sounding Solar and Stellar Interiors, ed. J. Provost, F. X. Schmider, & G. Berthomieu (Dordrecht: Kluwer), in press
Chou, H.-Y. 1994, M.S. thesis, Tsing Hua Univ.
Christensen-Dalsgaard, J., Schou, J., & Thompson, M. J. 1990, MNRAS, 242, 353
Fan, Y., Braun, D. C., & Chou, D.-Y. 1995, ApJ, 451, 877
Gough, D. O., & Thompson, M. J. 1991, in Solar Interior and Atmosphere, ed. A. N. Cox et al. (Tucson: Univ. Arizona Press), 519
Pijpers, F. P., & Thompson, M. J. 1992, A&A, 262, L33